OSAKA UNIVERSITY

A Study of Weak Nuclear Response by Nuclear Muon Capture

A thesis submitted in partial fulfillment
for the degree of

Doctor of Philosophy

by

IZYAN HAZWANI BINTI HASHIM

in the
Department of Physics
Graduate School of Science

December 2014

Abstract

Nuclear matrix elements (NMEs) for double beta decays (DBD) are crucial for extracting fundamental neutrino properties from DBD experiments. In order to study the DBD NMEs, single β^+ and β^- NMEs are required. The present research developed an experimental approach towards the determination of weak nuclear response (square of the NME) for the importance of fundamental properties of neutrinos. Hence, the present research aims at experimental studies of muon capture strength distributions, the β^+ side responses, to help/confirm theoretical evaluation for DBD NMEs.

Nuclear muon capture induced the excitation of the nucleus by compound nuclear formation and de-excitation of the compound nucleus by neutron emission. However, captures on the excited states of nucleus are preferable in comparison with capture on the ground state. The gamma rays accompanied the neutron emission is from the transitions from an excited state to the ground state. The production of isotope after muon capture evaluated the capture strength via observation of nuclear gamma rays and X-rays. We used the enriched molybdenum thin film in our first measurement at J-PARC, MLF.

The statistical neutron decay calculator explained the theoretical approach with the limitation to the excitation energy which corresponds to the Q-value of muon captures. Neutron binding energy is the threshold energy for emission of neutron and their cascade process after nuclear excitation is explained by emission of the fast pre-equilibrium neutrons(PEQ) and evaporating neutrons(EQ) fraction.

The second part discusses the experimental observation of isotope production after (μ,xn) reaction on ^{100}Mo target with x = 0,1,2, ... neutron emission. The isotopes are identified by their gamma-rays following the capture reaction and the observed half-life from the decay curve.

The final phase elaborates the comparison of previous feasibility test on ^{Nat}Mo and the current ^{100}Mo experimental observations with the neutron statistical calculations for both natural and enriched Molybdenum targets. From the population of isotopes produced by the reaction, one may get the muon-capture strength distribution, which can be used to help deduce the nuclear responses relevant to neutrino less double beta decays.

Acknowledgements

It is my exquisite pleasure to consummate doctor course and take a degree of Doctor of Philosophy in Osaka University. I would like to express my gratitude here to many people supported this accomplishment for over 3 years of my stay.

First, I would like to show my greatest appreciation to Prof. Yoshitaka Kuno who is my supervisor for the valuable advices and persistent helps from him to ameliorate my study. My deepest appreciation goes to Prof. Hiroyasu Ejiri who first suggested the muon capture reaction for the study of neutrino-less double beta decay. He lets me know how interesting particle physics is. His valuable discussions, advices, and incisive comments help me a lot in my study and experiment. My heartiest thanks to Associate Prof. Akira Sato who taught me how to perform the experiments and helping out in completing the details of the analysis. Associate Prof. Tatsushi Shima and Dr. Keiji Takahisa supported me in RCNP, Osaka University. Their technical advice, educational comments and useful feedbacks have been a great help to me to understand and operate the detectors and apparatus on-site.

I would like to thank the collaborators in MuCID, Dr Hideyuki Sakamoto, Associate Prof. Kazuhiko Ninomiya, Prof. Atsushi Shinohara, Yuko Hino, Nguyen Duy Thong and Nam Tran Hoai. Under their mentorships, I learnt many things besides physics. My intellectual debt is especially dedicated to Dr. Itahashi Takahisa who helped and supported me in the analytical processes. In addition, my life in Osaka has been enjoyable together with them and also the students in Kuno Laboratory. These three years has been a great pleasure, priceless and precious memory. I will always treasure them in my life.

I am also gratefully appreciate the financial support of UTM and KPM that made it possible for me to complete my challenge.

Finally, I would like to express my gratitudes to my husband and family for their moral supports and encouragements.

Contents

Abstract ii

Acknowledgements iii

List of Figures vi

1 Introduction 1
- 1.1 Neutrino Physics . . . 1
  - 1.1.1 Dirac and Majorana Neutrino . . . 2
  - 1.1.2 Neutrino Mass Beyond the Standard Model . . . 4
- 1.2 Neutrinoless Double Beta Decay . . . 5
- 1.3 Neutrino Nuclear Responses . . . 8
  - 1.3.1 Experimental Probes for the Nuclear Responses Studies . . . 9
  - 1.3.2 β^+ Nuclear Responses Studies . . . 11
- 1.4 Outline of This Thesis . . . 12

2 Muon Probe Responses 13
- 2.1 Muon Capture Reaction . . . 13
  - 2.1.1 Formation Of Muonic Atom . . . 14
  - 2.1.2 Muon Decay and Cascade Process . . . 16
    - 2.1.2.1 Neutron Emission . . . 17
  - 2.1.3 Muon Activation Analysis . . . 17
  - 2.1.4 Reaction Cross Section . . . 18
  - 2.1.5 Beta Strength Distribution . . . 18
  - 2.1.6 Gamma Rays Analysis . . . 19
    - 2.1.6.1 Calibration . . . 19
    - 2.1.6.2 Efficiency Correction . . . 19
    - 2.1.6.3 Nuclear Gamma Cascade Effect . . . 19
  - 2.1.7 Beta Decay Half Life . . . 20
- 2.2 Feasibility Test at MuSIC Facility . . . 21
- 2.3 Overview of This Method . . . 22

3 Experimental Instruments and Procedures 23
- 3.1 Beam Course . . . 23
- 3.2 Gamma detectors and shielding . . . 25
- 3.3 Data taking system . . . 26

3.4 Experiment setup . . . 26

4 Experimental Results **28**
4.1 Energy Calibration . . . 28
4.2 Detector efficiency . . . 30
4.3 Delayed Gamma-ray spectrum . . . 31
4.4 Gamma rays from ^{99}Mo . . . 34
4.5 Gamma rays from ^{98}Nb and ^{98}Nb . . . 36
4.6 Gamma rays from ^{97}Nb . . . 37
4.7 Gamma rays from ^{96}Nb . . . 37
4.8 Upper limit of ^{95}Nb . . . 39
4.9 Relative population of isotope . . . 39
4.10 Isotope Production, R(X') . . . 41

5 Neutron Emission Statistical Model **43**
5.1 Basic Principles and Assumption . . . 43
5.2 Initial Excitation Energy, E_0^{ex} . . . 46
5.3 Excitation Energy, E_i^{ex} . . . 47
5.4 Neutron Kinetic Energy Distribution, E_i^N . . . 47
5.5 Population of low-lying levels . . . 49
5.6 Performance of Neutron Statistical Model . . . 50

6 Comparison with the Neutron Statistical Model calculations using various Capture-Strength Distributions **53**

7 Discussion and Concluding Remarks **61**
7.1 Achievements . . . 61
7.1.1 Relative Weak Strength . . . 61
7.2 Issues . . . 63
7.2.1 Pile-up problems in short lived nuclei of ^{100}Nb, ^{99}Nb and X-rays measurement . . . 63
7.3 Future Prospects . . . 65
7.3.1 The new MuSIC beam line . . . 65
7.3.2 Prospects to deduce NME using ^{100}Mo data . . . 66
7.3.3 Future Plan . . . 66
7.4 Application of Muon Capture Reaction . . . 67
7.5 Summary . . . 67

A Appendix A: Geant 4 Simulation **69**

B Appendix B: Energy calibration Source **71**

C Appendix C: Properties of Radio Isotopes **73**

Bibliography **78**

List of Figures

1.1 Neutrino mass hierarchy[12] . . . 4
1.2 Level diagram for double beta decay reaction . . . 5
1.3 Schematic diagram of two neutrino and neutrino less double beta decay experiment [3][21] . . . 6
1.4 Double beta and single beta response probe[24] . . . 10
1.5 Nuclear response probe[2][21] . . . 10

2.1 Gamma branching and magnetic (M1, M2, M3, M4) and electric quadrupole (E1, E2, E3) interactions was shown at each corresponding gamma energy[44]. . . . 15
2.2 Example of gamma-decay scheme . . . 20
2.3 Gamma rays spectrum from feasibility test at MuSIC facility[7][20]. . . . 21

3.1 Double pulse structure of MLF Facility . . . 24
3.2 (a)Muon section at MLF-JPARC (b)D2 beam line at MLF-JPARC . . . 24
3.3 D2 muon beam intensity at 220kW[26] . . . 25
3.4 Muon irradiation at D2 . . . 27
3.5 Trigger logic for D2 beam test . . . 27

4.1 Peak assignment from delayed spectrum . . . 28
4.2 Energy calibration (a) Run1 (b) Run2 . . . 29
4.3 Consistency check with peak width (a) free (b) fixed parameter . . . 30
4.4 Efficiency curve by simulation . . . 31
4.5 Energy spectra for off beam measurement . . . 32
4.6 Delayed gamma spectra from off beam measurement . . . 33
4.7 Decay curve of 140.5keV . . . 34
4.8 Decay curve of (a)181.1keV (b)739.5keV . . . 35
4.9 Decay curve of (a)722.6keV (b)787.4keV . . . 36
4.10 Decay curve of 657.9keV . . . 37
4.11 Decay curve of (a)460keV (b)569keV (c)778keV . . . 38
4.12 Decay curve with fixed half life (a)140.5keV (b)181.1keV (c)739.5keV (d)722.6keV (e)787.4keV (f)657.9keV (g)460keV (h)569keV (i)778keV . . . 40
4.13 Capture strength distribution from muon capture reaction on ^{100}Mo . . . 42

5.1 Momentum balance after the beta decay of a nucleus . . . 44
5.2 Layout of neutron statistical model with muon captures on target nuclei and emission of x neutrons . . . 44
5.3 Excitation energy distribution of the statistical calculator . . . 46
5.4 Excitation energy spectrum for ^{100}Mo . . . 47

5.5 Distribution of neutron kinetic energy of the statistical calculator 48
5.6 Neutron energy spectrum for ^{100}Mo (a) 15 percent of PEQ event (2) 22 percent of PEQ event (c) 32 percent of PEQ event 48
5.7 Isotope population distribution of the statistical calculator 49
5.8 Initial excitation energy with energy difference 5MeV 51
5.10 Average isotope population for corresponding nuclear excitation 51
5.9 Raw population distribution when nuclear excitation from 5 to 50MeV . . 52

6.1 Model A: Nuclear excitation energy fraction and comparison model A with experimental observation by 100 Mo 54
6.2 Model B: Nuclear excitation energy fraction and comparison model B with experimental observation by 100 Mo 55
6.3 Model C: Nuclear excitation energy fraction and comparison model C with experimental observation by 100 Mo 56
6.4 Model D: Nuclear excitation energy fraction and comparison model D with experimental observation by 100 Mo 57
6.5 Model E: Nuclear excitation energy fraction and comparison model E with experimental observation by 100 Mo 58

7.1 Energy spectra for on beam measurement 63
7.2 The new MuSIC beam line at RCNP, Osaka University 65

A.1 Geant 4 simulation estimation of probability of muon stopping, acceptance and peak efficiency. 69

B.1 Calibration source for MLF measurement 72

C.1 Level diagram of ^{100}Mo[50] 73
C.2 Level diagram of ^{100m}Mo[50] 74
C.3 Level diagram of ^{99}Mo [43] 74
C.4 Level diagram of ^{98}Mo [39] 75
C.5 Level diagram of ^{97}Mo [40] 76
C.6 Level diagram of ^{96}Mo [41] 76
C.7 Level diagram of (a) ^{95}Mo (b)^{95m}Mo [42 77

Chapter 1

Introduction

The study of neutrino fundamental properties are crucial because of its neutral charge and unknown mass. In a radioactive decay, W.Pauli has observed a non-conserved energy apparent energy which contributed to the postulation of neutrino as a neutral particle. The discovery of neutrino 20 years later at the nuclear reactor augmented the interest to study the basic properties of neutrino [1]. The fundamental properties of neutrino and astro-neutrino nuclear interactions studied by single β decay, $\beta\beta$ decay, the inverse β decay and neutral current nuclear excitations experiments.

Up till now, the accord of neutrino properties such as its mass hierarchy, or it's characterised as Majorana or Dirac neutrino etc. are still ambiguous resulting from the unknown absolute neutrino mass scale. This mass scale information procured from the transition rate of $0\nu\beta\beta$ decay experiment. However, this experiment is beyond the standard model(SM) and a very rare process. Moreover, the accurate value of the coupling constant and correlation parameters are not well known causes the nuclear matrix element(NME) to be undetermined.

This research report will provides the new information for the NME by studying the β^+ side of the double beta decay (DBD) using the nuclear muon capture reaction. We aim to provide the theorist the strength distribution of muon capture reaction for understanding the coupling constants and correlation parameters relevant to DBD experiments. This chapter will briefly explains the neutrino physics background, experimental probes for the neutrino studies and the advantages of weak nuclear probes.

1.1 Neutrino Physics

Neutrinos passing through the universe like a mere spectators. Their discovery become unnoticed due to their ability to travel through the earth without any interaction. Even though, after half a century, we still know less about them. Once the interaction between a neutrino and weak force known as the weak interaction was realised, neutrino has an insignificant gamble of interacting with anything.

In 1930, W.Pauli proposed that the apparent violation of energy and momentum conservation can be easily avoided by postulating another particle produced along with the electron in beta decay. This elusive particle has no charge like neutron, almost no mass

and has 1/2 spin. In three years later E. Fermi [2] developed a beta decay theory based on the interaction between neutrino and other particles.

$$n \rightarrow p + e^{-} + \bar{\nu}_e \tag{1.1}$$

E.Fermi established the theoretical equations of beta decay by assuming the neutrino mass is zero considering the empirical energy spectrum of decay electron. The zero mass neutrino was introduced into the SM. Their existence was unknown until 1956, after Clyde Cowan and Fred Reines performed an experiment at nuclear reactor [3]. Their experiment observed the cross sections of inverse beta decay of protons from fission fragment [1].

Later in 1962, L. M. Lederman, M. Schwartz and J. Steinberger detected the interactions of muon neutrino by spark chamber experiment. They concluded that there were more than one type of neutrinos exists. Fundamental properties of neutrino was aggressively studied since 1970s by double beta decay experiment, inverse beta decay and neutral current nuclear excitations [3] [1]. Consequently, the heaviest tau neutrino was discovered on 2000 by DONUT. The intense neutrino beam was fired on a target consists of iron plates with layers of emulsion sandwiched between them to produce tau lepton which then subsequently decayed by leaving a characteristic track in the emulsion.

1.1.1 Dirac and Majorana Neutrino

In the SM framework, $2\nu\beta\beta$ decays are followed by two neutrino and anti-neutrino and thus the lepton number is conserved. Meanwhile, the $0\nu\beta\beta$ decays violated the lepton number conservation law by ΔL=2 with the decay associated with neutrinos and weak interaction beyond the SM. Majorana neutrino assume that the have masses and neutrino and anti neutrino posses the same energy. In order to establish that neutrino is a Majorana particle, one requires a measurement of decay rate, the data of neutrino oscillation and a good and reliable calculation of nuclear matrix element is very important [4] [5] [6]. However, it is important to clearly know the nuclear matrix element of the transition to yield the neutrino mass Eigen states and gives accurate information about nuclear structure. From Majorana and Dirac neutrino description, a mathematical representation is necessary to explain a peculiarity which does not exist in case of charged fermions.

Until 1995, only ν_L and $\bar{\nu}_R$ have been detected experimentally. The spin and momentum remain constant by charge conjugation, thus ν_L does not corresponds to the $\bar{\nu}_R$. However, they were related by CP operation which was responsible for the change of the sign of handedness $\nu_L^{CP} = \bar{\nu}_R$. In relativistic quantum theories, half integral spin fermions were described by 4 components spinor which gave solution to Dirac equation. The following mass term of Dirac and Majorana neutrinos are summarised from [7].

The left and right handed components of $\psi(x)$ are easily obtained by applying the P_L and P_R

$$\psi_L = P_L \psi \tag{1.2}$$

$$\psi_R = P_R \psi \tag{1.3}$$

The four components of Dirac field $\psi(x)$ is the sum of the Weyl Spinors (ψ_L and ψ_R) and the Dirac's field is represent by the following equation.

$$\psi(x) = \sum_{S=L,R} \int \frac{d^3p}{\sqrt{2\pi^2}2E}(b_S(p)u_S(p)e^{-ipx} + d_S^+(p)\nu_S(p)e^{ipx}), \tag{1.4}$$

b_S and d_S^+ were the annihilation operators and their corresponding creation operators, while u_S and ν_S were independent basic spinors.

Assuming that ν_R existed and they are distinguishable as ν_R^C. The four components of Dirac particle can be written as

$$\nu_D = \nu_L + \nu_R \tag{1.5}$$

and

$$\nu_D^C = \nu_L^C + \nu_R^C \tag{1.6}$$

In Lagrange density derived from the Euler-Lagrange equation is expressed in term of mass of different helicities and simplify hermitian conjugate.

$$\mathcal{L}_D = m^D \bar{\nu}_L \nu_R + h.c = m^D \bar{\nu}_D \nu_D \tag{1.7}$$

The Dirac equation is divided into 2 coupled equations with 2 fields with different handedness where Dirac mass, m_D denotes the coupling strength.

Majorana neutrino introduced different types of coupling for the case of electrically neutral neutrino. If ν_R and ν_R^C are physically indistinguishable, two components theory of neutrino are resolves from Dirac equation. There are 2 Majorana mass term corresponds to the left and right handed field with their CP conjugate.

$$\mathcal{L}_M = \mathcal{L}_M^L + \mathcal{L}_M^R \tag{1.8}$$

where

$$-\mathcal{L}_M^L = \frac{1}{2} m_L^M (\bar{\nu}_L \nu_R^C + \bar{\nu_R^C} \nu_L) \tag{1.9}$$

$$-\mathcal{L}_M^R = \frac{1}{2} m_R^M (\bar{\nu}_R \nu_L^C + \bar{\nu_L^C} \nu_R) \tag{1.10}$$

All ν_L and ν_R^C with their conjugate ν_R and ν_L^C are combined into Majorana mass eigenstates ν_1 and ν_2 which are their own antiparticle. The Lagrange density can be rewrite in terms of ν_1 and ν_2

$$-\mathcal{L}_M^L = \frac{1}{2} m_L^M (\bar{\nu}_1 \nu_1) \tag{1.11}$$

and vice versa.

Majorana case can be distinguished from Dirac case when:
a) the mass term m=0 causes either 2 or four degrees of freedom are detectable.
b) for massive neutrino, the magnetic moment are indicates from CPT theorem due to opposite signs of neutrino and antineutrino.

1.1.2 Neutrino Mass Beyond the Standard Model

The standard model of particle physics assumes that neutrinos are massless. In order for neutrino oscillations to occur, some neutrinos must have masses. Therefore, the standard model of particle physics must be revised. There are two possible types of neutrino oscillation experiments. The first is to start with a pure beam of known flavour ν_x, and look to see how many have disappeared. This is a "disappearance" experiment and measured the survival probability:

$$P(\nu_x \to \nu_x) = 1 - sin^2(2\theta) \times 1.27 sin^2 \Delta m^2 \frac{L}{E} \tag{1.12}$$

where Δm^2 is the squared mass difference and L/E is the control parameter for the distance between source and the detector and the energy of neutrino. The second type of experiment is an "appearance" experiment, which starts with a pure beam of known flavour ν_x and to see how many neutrinos of a different flavour ν_y are detected. The values of the different neutrino masses may be clues that lead to understanding physics beyond the standard model of particle physics. Assuming there are 2 flavours involve, there will be 2 mass states. This parameter is the difference in squared masses of each of these states:

$$\Delta m^2 = m_1^2 - m_2^2. \tag{1.13}$$

For neutrino oscillations to occur, at least one of the mass states must be non-zero. This simple statement gives huge implications that in order for oscillations to happen, the neutrino must have mass. Furthermore the masses of the mass states must be different, else $\Delta m^2 = 0$ and $P(\nu_x \to \nu_y) = 0$. We can see that the masses control the relative phase of the two mass wave functions.

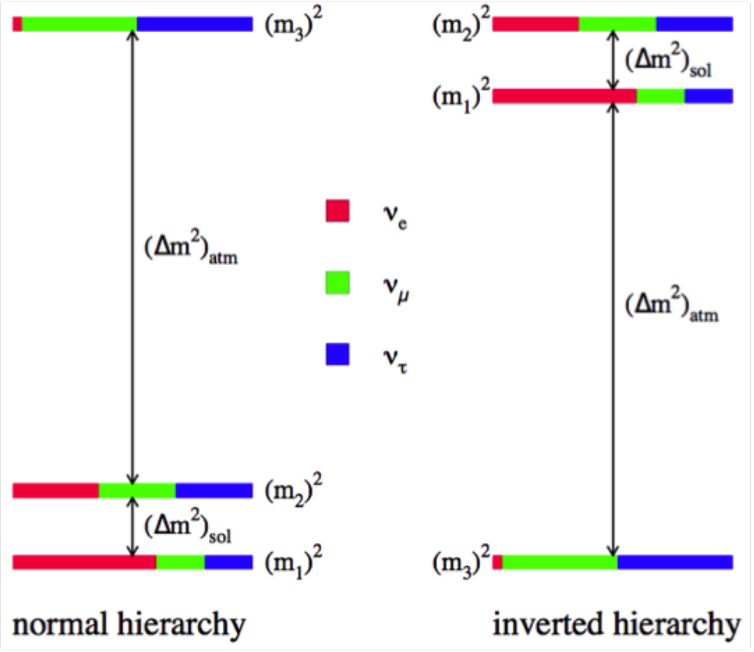

FIGURE 1.1: Neutrino mass hierarchy[12]

There are limitation of neutrino oscillation experiments, they can give us detailed information on the squared mass difference values, but cannot tell us what the absolute mass of the corresponding states. Neither can they tell us whether m_1 is larger in mass than m_2. If $\Delta m^2 \rightarrow -\Delta m^2$ the probability will still be the same. The relations between the mass description and the associated-particle description involved certain constants, called "mixing angles", whose values are potentially important clues that may help lead to an improved theory of how elementary particles behave [8].

The magnitude of the mass-squared splitting between states ν_1 and ν_2 is known from the KamLAND reactor experiment, and the much larger mass splitting between the third, ν_3 state and the ν_1 - ν_2 pair is known from atmospheric and long-baseline experiments. However, pure neutrino oscillations are sensitive only to the magnitude of the mass splitting, not the sign. Defining the ν_1 state as having the largest admixture of the electron flavor eigenstate, the sign of the mass splitting between states ν_2 and ν_1 is determined to be positive ($\Delta m^2_{21} > 0$) using the pattern of neutrino oscillations through the varying-density solar medium. However, the corresponding sign of $\Delta m^2_{32} \approx \Delta m^2_{31}$ remains unknown. There are two potential orderings for the neutrino mass the "normal hierarchy", which showed ν_3 is the heaviest, and the "inverted hierarchy", which showed ν_3 is the lightest. This is illustrated in figure 1.1.

1.2 Neutrinoless Double Beta Decay

The doubt of neutrino masses and mixing is one of the most important issues of modern particle physics. One of the method to study the fundamental properties of neutrino is by double beta decay, a rare nuclear process observable in even-even nuclei. The ordinary beta decay is energetically forbidden or highly suppressed by large spin differences. An initial nucleus X(Z, A) decays to X"(Z+2, A), emitting two electrons in the process. The level diagram shows in figure 1.2 of nucleus X'(Z+1, A) is higher than that of the initial nucleus, and it is forbidden to decay.

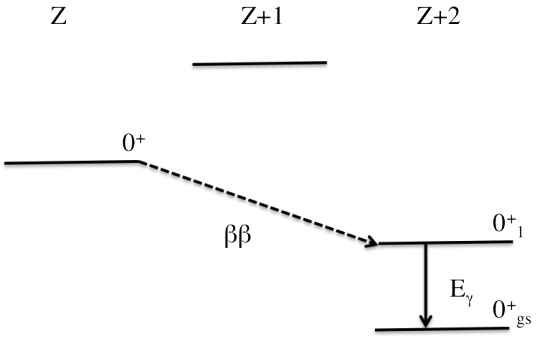

FIGURE 1.2: Level diagram for double beta decay reaction

About a year after Fermi introduced the idea of weak interaction theory, Maria Goeppert-Mayer published an article about double beta decay, $\beta\beta$. In the publication, she derived $2\nu\beta\beta$ transition rate and the half-life of the decay are estimated, assuming that the Q-value is 10MeV.

$$ {}^{A}_{Z}X \rightarrow {}^{A}_{Z+2}X" + e^- + e^- + \bar{\nu}_e + \bar{\nu}_e \tag{1.14} $$

Fireman reported the first observation of $\beta\beta$ decay of ^{124}Sn in laboratory experiment in 1949, however he disclaimed it later. So far, 35 nuclei has been recorded as candidate of $\beta\beta$ decay but most popular nuclei used by major DBD experiments are ^{48}Ca, ^{76}Ge, ^{82}Se, ^{96}Zr, ^{100}Mo, ^{116}Cd, ^{130}Te, ^{128}Te, ^{150}Nd, ^{136}Xe and ^{238}U. The process of $\beta\beta$ decay is experimentally demonstrated over a period of more than 20 years.

In 1937, Ettore Majorana formulated a new theory about neutrino where the neutrino and antineutrino are indistinguishable. He suggested antineutrino induced β^- decay for experimental verification.

$$\nu + {}^{A'}_{Z'}X \rightarrow {}^{A'}_{Z'+1}X' + e^- \tag{1.15}$$

Here we will describe briefly the theory of $\beta\beta$ decay referring to explanation and elaboration by [6] and [4]. The schematic diagram of two neutrino double beta decay and neutrino less double beta decay is shown in Figure 1.3 which illustrated the difference mechanism occured during the decay process where A: $2\nu\beta\beta$. B: $0\nu\beta\beta$ with single Majoron emission. C: $0\nu\beta\beta$ with Majorana neutrino exchange. D:$0\nu\beta\beta$ with SUSY particle exchange.

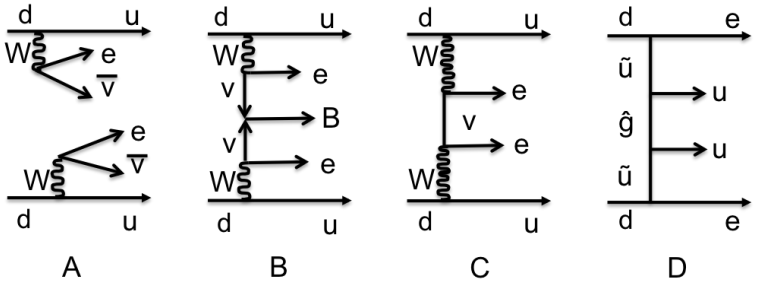

FIGURE 1.3: Schematic diagram of two neutrino and neutrino less double beta decay experiment [3][21]

In later description, T represents the transition rate(probability), $M^{0\nu}$ is the nuclear matrix element, $G^{0\nu}$ is the kinematical factor including the phase space volume and double weak coupling constant. The transition rate for $\beta\beta$ decay is simply expressed in terms of $M^{2\nu}$ and $G^{2\nu}$. The $2\nu\beta\beta$ is a four body process with fixed total energy of $Q_{\beta\beta}$. The rate of $2\nu\beta\beta$ increased rapidly with the increment of $Q_{\beta\beta}$ since the Coulomb effect favours $\beta^-\beta^-$ rates at higher Z nuclei(most of double beta decay candidates are medium or heavy nucleus).

$$T^{2\nu} = G^{2\nu}|M^{2\nu}|^2 \tag{1.16}$$

The transitions in $2\nu\beta\beta$ are mainly Gamow Teller (GT) type since beta rays are mostly low-energy s-wave electrons. The important coupling constant $(g_A G_F cos\theta_C)^4$ given by axial parameter, g_A, Fermi coupling constant, G_F and θ_C as the Cabibbo angle. From the allowed GT($\tau\sigma\tau\sigma$) and Fermi ($\tau\tau$) matrix element, the nuclear matrix element, $M^{2\nu}$ can be deduced.

In the case of light Majorana neutrino emission, one neutron is reabsorbed by the other neutron of the same nucleus. This process requires coexistence of left and right hand

helicity which is relevant with weak Hamiltonian symmetric model. the $j_{L\mu}$ and $J_{L\mu}$ indicated the left-handed lepton and hadron current and the subscripts of R indicate the term for right handed.

$$H = G_F cos(\theta_C)(2)^{-1/2}[j_{L\mu}J^+_{L\mu} + \chi j_{L\mu}J^+_{R\mu} + \eta j_{R\mu}J^+_{L\mu} + \lambda j_{R\mu}J^+_{R\mu}] + h.c. \tag{1.17}$$

The first term is the neutrino mass term and the following terms associate with the right handed weak interaction where interaction coefficients (χ, η, λ) are given by the θ_{LR} between left and right W bosons (W_L and W_R) and their respective masses term.

$$\chi = \eta \approx -tan\theta_{LR}, \lambda \approx (\frac{M_L}{M_R})^2 \tag{1.18}$$

The left and right handed eigenstate neutrino ν is expressed in mass eigenstate, ν^m are

$$\nu_L = U\nu^m_L, \nu_R = V\nu^m_R \tag{1.19}$$

In different case, the neutrino less double beta decay transition deduced from $T^{0\nu}$=$\frac{ln2}{T^{0\nu}_{1/2}}$ is expressed with particular $M^{0\nu}$ which is the nuclear matrix element, while $G^{0\nu}$ is the kinematical factor for the decay. The current $G^{0\nu}$ is smaller by a factor of ln 2 than the kinematic factors for the inverse half-life.

$$T^{0\nu} = G^{0\nu}|M^{0\nu}|^2 K_{\nu R} \tag{1.20}$$

where $K_{\nu R}$ stands for the neutrino mass and right handed current term which deduce the neutrino mass effective terms. They are expressed as

$$\begin{aligned} K_{\nu R} = [(\frac{< m_\nu >}{m_e})^2 + C_{\lambda\lambda} < \lambda >^2 + C_{\eta\eta} < \eta >^2 + C_{m\lambda}\frac{< m_\nu >}{m_e} < \lambda > cos\psi_1 \\ + C_{m\eta}\frac{< m_\nu >}{m_e} < \eta > cos\psi_2 + C_{\eta\lambda} < \lambda >< \eta > cos(\psi_1 - \psi_2)] \end{aligned} \tag{1.21}$$

$$< m_\nu >= |\Sigma m_j U^2_{ej}| \tag{1.22}$$

$$< \lambda >= \lambda|\Sigma U_{ej}V_{ej}| \tag{1.23}$$

$$< \eta >= \eta|\Sigma U_{ej}V_{ej}| \tag{1.24}$$

In the study of $0\nu\beta\beta$, the effective mass terms are expressed in terms of the neutrino mixing coefficients and the absolute mass of the eigenstates. The neutrino oscillation data provides the mass-square differences and the mixing coefficients. The neutrino flavour eigenstates and the mass eigenstates is connected by the mixing matrices U and V. In light Majorana-ν mass left handed weak current term explicitly expressed by Majorana phase matrix U_p as $U = U_m U_p$. Finally the $0\nu\beta\beta$ rate simply written as $T^{0\nu} = G^{0\nu}|M^{2\nu}|^2| < m_\nu > |^2$ and the effective mass term is $< m_\nu >= |\Sigma|U_{ei}|^2 m_i e^{i\alpha_i}|$.

1.3 Neutrino Nuclear Responses

There are several ways to determine the NME, either experimentally tested by direct kinematical approach through nuclear beta decay and double beta decay experiments or theoretical approach by evaluation from various calculation models. The neutrino nuclear response is equal to the square of NME but we can not deduce the phase of NME due to the square value. The effective mass of neutrino is extracted from the transition rate of double beta decay experiment. The NME has contribution from the axial coupling constant, g_A and nuclear spin-isospin correlation parameter, g_V and theoretical model dependent. The uncertainty of NME is quite large due to these not well known parameters.

The early study of double beta decay structure calculations are mostly focused by using the nuclear shell model as a commencement point. Shell model has some limitation to only single particle motion in bound orbitals in response to the remainder of the system. In theoretical description of double beta decay process proceed through intermediate double-odd nucleus virtual states [9] [4]. The extreme single particle model works well near the vicinity of closed shell, but requires more approximations as we move to several nucleons away from the major closed shell. Pauli Exclusion Principle provides a little philosophical support for proceeding with development of such a model.

The entrance of the different energies on the nucleons of different angular momentum states. Hence causes the nucleus to move in a harmonious fashion, to avoid suffering from frequent collisions. However, it still remains in the discrete orbitals for the validity of the model [10] [11]. The saturation of nuclear forces resulting in an approximate constant binding energy for each constituent nucleon, independent of the details of nuclear structure. This is attributed to the fact that the size of the nucleus is basically proportional to the number of nucleons and hence the nucleus seems to be a rather compact object with nucleons basically touching each other.

Due to the fact that double beta decay nuclei are mostly medium-heavy nuclei or heavy nuclei, a more suitable Quasiparticle Random Phase Approximation (QRPA) have been introduced [12]. Compare to the nuclear shell model, QRPA and pn-QRPA are malleable in heavy nuclei. An adjustable parameter for the proton-neutron interaction, g_{pp} is introduced. The half-life of double beta decay are sometimes strongly depends on the strength parameter g_{pp}. Experiments such as muon capture observables [9] and renormalizing pn-QRPA [13] are some suggested experiments in order to fix g_{pp} parameter.

The $2\nu\beta\beta$ decay ensues from the grandfather nucleus to the daughter nucleus through the 1^+ states of the intermediate nucleus. The corresponding half-life of this decay is factorised by

$$T^{2\nu}_{1/2}(T^+_i \rightarrow T^+_f) = [G^{2\nu}|M^{2\nu}|^2]^{-1} \tag{1.25}$$

It has been emphasised by previous report of Kortelainen [10], that the Ordinary Muon Capture (OMC) probes for double beta decay only involved one of the two branches $\beta\beta$ decay in a 2 stepped process. From his observation, the total and partial capture rates give enough information about the nuclear structure of intermediate nuclei of any $\beta\beta$ decay candidates. The similar information is also concluded then by log ft value.

Until the 20^{th} centuries, the direct determination covers all nuclear β decays resulting $\bar{\nu}_e$ from β^- decay and ν_e from β^+ decay or EC. These reaction is closely related to the neutrino capture reactions. The Q-value indicates the mass differences between mother and daughter nucleus, where Q-value $\nleq 0$. The β^+ decay and EC leads to the daughter nucleus with same Z.

β^+ decay:

$$Q_{\beta+} = [m(Z, A) - m(Z - 1, A) - 2m_e]c^2 \tag{1.26}$$

Electron Capture:

$$Q_{\beta+} = [m(Z, A) - m(Z - 1, A)]c^2 \tag{1.27}$$

The probing by electron capture and beta decay only gives the information of the lowest J^π state of the odd-odd nuclei. By muon capture reaction which is relatively known having a higher momentum transfer due to it's mass is 203 times heavier than the electron might probe higher J^π state of the intermediate nuclei. This gives more accurate information to the nuclear structure study of double beta decay.

Nuclear responses for $\beta\beta$ decay are important for neutrino studies in nuclei. The nuclear response are very sensitive to spin isospin interactions and spin isospin correlations. Nuclear matrix element for $2\nu\beta\beta$ decay, $|M^{2\nu}|^2$ have been obtained by half life measurement. The current $|M^{2\nu}|^2$ are only in the order of 10^{-1} to 10^{-2} in units of $(\mathrm{m}_e)^{-1}$. The observed $2\nu\beta\beta$ matrix element are suppressed due to possible double GT transition at high excitation region but the value is not so much scattered. In 2002, Ejiri [5] suggested to include the nuclear medium effect on $2\nu\beta\beta$ response and also the future response of $0\nu\beta\beta$. Since the single response is the square of the matrix element, the expected range of single response is only in order of 10^{-2} to 10^{-3}.

1.3.1 Experimental Probes for the Nuclear Responses Studies

The determinations of the nuclear matrix element have been widely studied and in the last few years the reliability of the calculations has considerably improved [4]. Nuclear matrix element is directly proportional to the double beta decay transition rate and can be given by the sum of products of single β^- and β^+ nuclear responses [14] [7]. The $\beta\beta$ decay experiment was developed to study the fundamental properties of neutrino either Dirac or Majorana particle by measuring the double beta decay reaction rates and the upper limits of the neutrino effective mass. The isotopic $\beta\beta$ decay candidates were observed experimentally by calorimetric or spectroscopic method.

However, many newly developed experiments, which study the single beta response by using weak, electromagnetic and strong interaction to accurately describe first and second beta decay involved in the reaction and also studying the intermediate nuclear structure. In comparison to the nuclear matrix element for $2\nu\beta\beta$ and $0\nu\beta\beta$ direct observation, single neutrino responses are more sensitive to the nuclear structures, $\tau\sigma$ correlation, proton-proton correlation, effective axial parameters and others. The value of current limit of nuclear matrix element from the giant resonance (GR) excitation which are mostly from Gamow Teller transitions are extremely small after renormalisation of g_A and other short range correlation [4] [14].

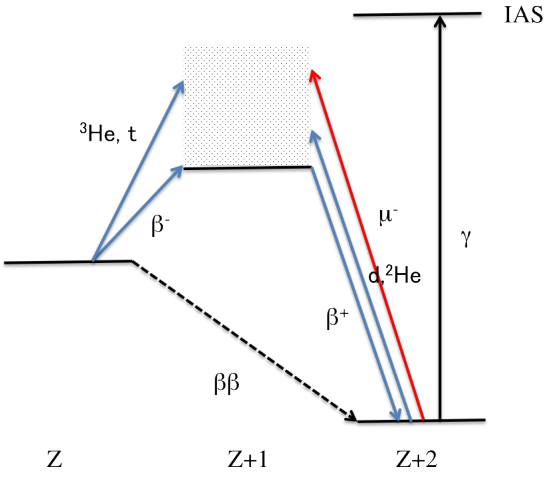

FIGURE 1.4: Double beta and single beta response probe[24]

Figure 1.4 shows the response from single and double beta decay experiments [15]. Double beta decay provide overall response from grandfather nucleus denotes as A to the daughter nucleus (B). While the single response such as nuclear β^- decay and charged exchange reaction by nuclear probe provides the β^- responses from nuclei A to C. Photo-absorption study by photon probes excites the nucleus until Isobaric Analog States(IAS) and gives nuclear structure of particular nuclear. Lastly, the weak probe and β^+ decay provides β^+ response of B and C nuclei.

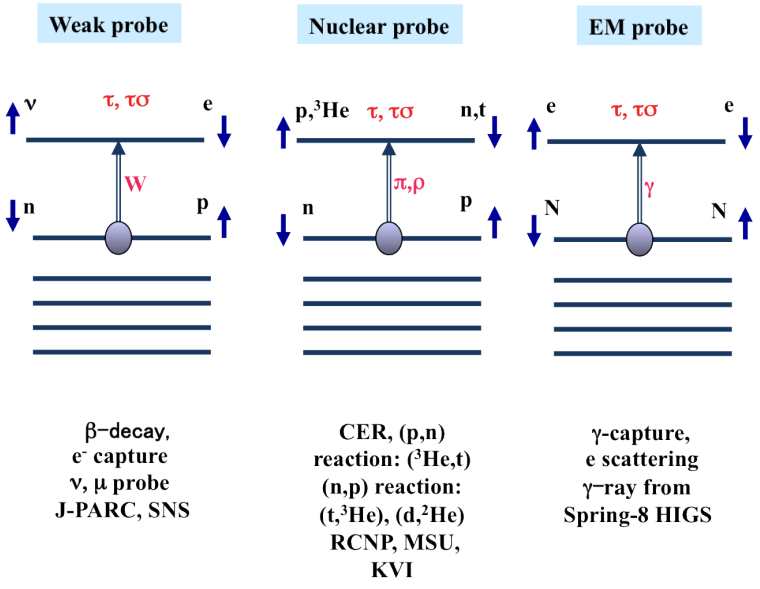

FIGURE 1.5: Nuclear response probe[2][21]

Nuclear and photon probes provides indirect approach towards the study of neutrino response. On the other hand, weak probe can comprehend the direct neutrino response. The nuclear probe gives high sensitivity measurement which accurately shows the 1^+ states of the excitation region it is a complimentary method to the weak probe. This method have been study at IUCF, KVI, RCNP and others to get the vector weak responses and axial-vector weak responses. The charge exchange reaction often studied by

(p,n), (n,p), (d,^{2}He), (^{3}He,t), (t,^{3}He) and (^{7}Li,^{7}Be) reaction. The cross section of charge exchange reaction is mainly due to large central isospin and spin-isospin interaction ($V_{\tau\sigma}$) and small distortion interaction (V_0) at medium energy.

Photo-nuclear reaction by electromagnetic probe through isobaric analog states (IASs) of target nuclei was recently study by many researchers. For a medium heavy nuclei, IAS was located on the E1 giant resonance (GR) in the range of high excitation region. Photo nuclear reaction includes isobaric analog resonance(IAR), GR and their interference term shown in equation below. The relative phase ϕ at IAR can be synthesised for matrix element determination. High energy electron are scattered from the laser photons are used during the photo nuclear reaction. The polarisation of the photon can be used to study E1 and M1 matrix element separately. New SUBARU and other electron synchrotrons is used to provide high intense laser electron photons for the photo-nuclear reaction.

The weak probe provides excitation region including 1^+, 1^-, 2^- and higher states by muon capture or neutrino interaction. We can hardly distinguish between these excitation region, however the higher 1^- and 2^- states can gives more information about the intermediate nuclei nuclear structure. In this study, we will demonstrate how lepton or weak probe is a very useful technique to determine the nuclear matrix element. It is best to study the weak interaction by neutrino itself, however due to unknown properties and characteristics of neutrino interaction give experimentalist the hard work. Investigation of nuclear weak interaction can also be done by lepton [4] [16]. It has been pointed in 1972 [14] and 2001 [17] that muon capture reactions are reliable to get the information on the β^+ side of DBD. RCNP, J-PARC and SNS are reliable facilities to provide high intense muon and neutrino beam for this reaction.

1.3.2 β^+ Nuclear Responses Studies

Instead of muon capture reaction, the (n,p) reaction such as (d,^{2}He) and (t,^{3}He) have also been used to study the β^+ responses for $\beta\beta$ decay. These reaction using deuteron and unstable triton beam provides information on the low lying states of nuclear structure especially the 0^+ and 1^+ states on particular nuclei. Due to the deuteron beam facility at KVI have been currently shut down, data on $\beta\beta$ decay nuclei can not be obtained.

Also previous work by muon capture reaction are focusing on light and medium nuclei which are not the candidate of $\beta\beta$ decay. Most of them are focusing on the comparison with zero neutron emission which in particular have the same outcome with (d,^{2}He) and (t,^{3}He) reaction. This type of reaction provides complicated structure resulting from the momentum transfer of muon capture which is high enough to excite high excited level.

In this present work, the results from muon capture reaction of ^{100}Mo will be presented. ^{100}Mo is the candidate for $\beta\beta$ decay which are used widely by several experiments such as Elegant, Osaka and NEMO III, but we should expect the β^+ response from ^{100}Ru nuclei. Due to it's typical mass number, we will study the β^+ response from ^{100}Mo. The whole excitation region by muon capture up to 50MeV which covers spin of 1^+, 2^- and so on will be discussed corresponds to the analysis of delayed RI gamma rays, which are very simple and clean.

1.4 Outline of This Thesis

The aim of this reports is to provide a new method of studying the NME for DBD by nuclear muon capture. In order to obtained these information, a new experimental techniques by nuclear muon capture is developed. The experimental data was evaluated by the first neutron statistical model for muon capture reaction. The relative muon capture strength will be deduced from the comparison of the statistical model and experimental results on ^{100}Mo.

This research report will be organise as follows, chapter 1 briefly explains the status of neutrino physics, experimental probes of neutrino responses and previous work on β^+ side of NME. The mechanism of muon capture, features of nuclear muon capture and its response for DBD NME estimation will be described in chapter 2. Chapter 3 will includes the detailed explanation of the development and performance of neutron statistical model. Further explanation on the methodology of the experiment and analysis will be emphasized in Chapter 4 and Chapter 5. Chapter 6 will showed the comparisons with suggested statistical model. The discussion regarding the problem faced during experiment and the analysis results and the concluding remarks are summarised in Chapter 7.

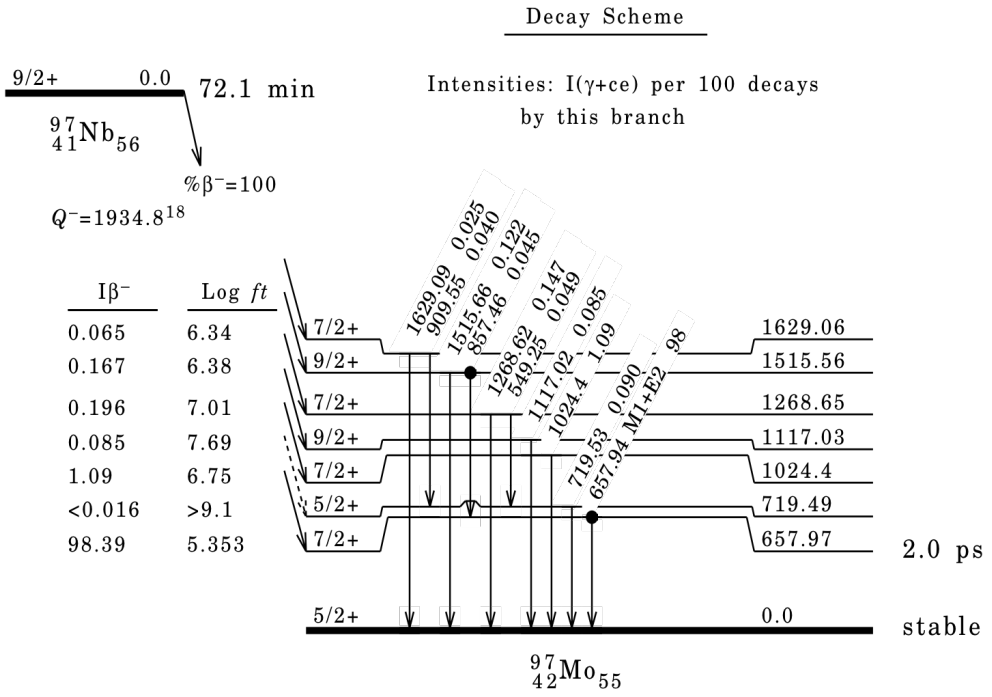

FIGURE C.5: Level diagram of ^{97}Mo [40]

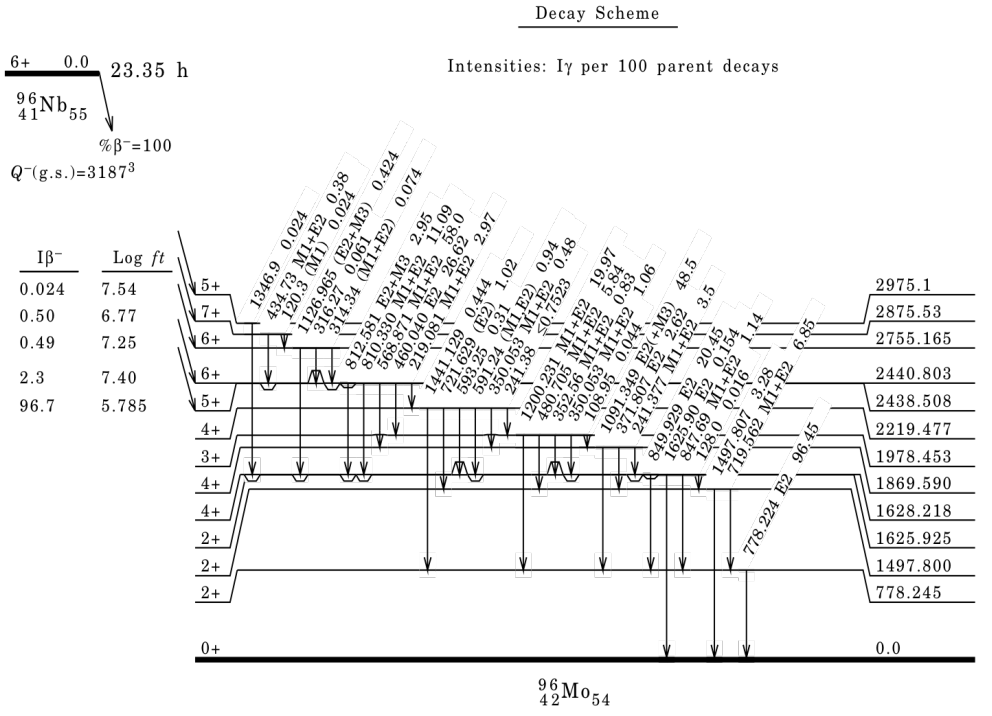

FIGURE C.6: Level diagram of ^{96}Mo [41]

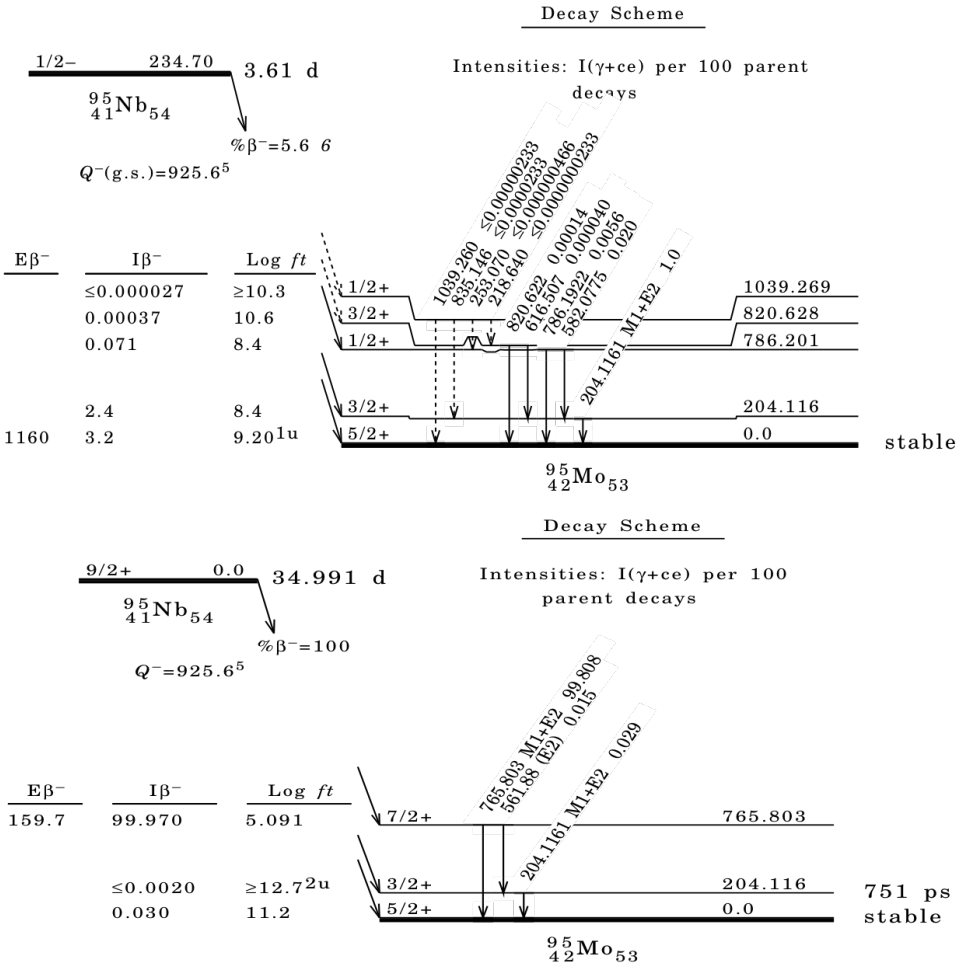

FIGURE C.7: Level diagram of (a) ^{95}Mo (b)^{95m}Mo [42

Bibliography

[1] F.Close. *Neutrino*. Oxford University Press, Oxford, NY, 2010.

[2] G.Rajasekaran. Fermi and the theory of weak interactions. *History and Philosophy of Physics*, 19(1):18–44, January 2014. URL http://arxiv.org/abs/1403.3309v1.

[3] F.Reines. A brief history of neutrino experiment at lampf. Los Alamos Science, 1997.

[4] J.D Vergados, F.Simkovic, and H.Ejiri. Theory of neutrino less double-beta decay. *Reports on Progress in Physics*, 75(10):1–52, September 2012. URL http://iopscience.iop.org/0034-4885/75/10/106301/.

[5] H.Ejiri. Double-beta decays and neutrino masses. *Progress in Particle and Nuclear Physics*, 48(00124):185–200, November 2002.

[6] H.Ejiri. Double beta decays and neutrino masses. *Journal of Physical Society of Japan*, 74(8):2101–2127, August 2005.

[7] H.V. Klapdor-Kleingrothaus and A. Staudt. *Non-accelerator Particle Physics*. Oxford Science Publications, Oxford, NY, 1998.

[8] H.Yoshida. *Limit on Majorana Neutrino Mass with Neutrinoless Double Beta Decay from KamLAND-Zen*. Tohoku, Japan, 2013.

[9] M. Kortelainen and J.Suhonen. Ordinary muon capture as a probe of virtual transitions of double beta decay. *Europhys. Letter*, (58):666–672, January 2002. URL http://arXiv:nucl-th/0201007.

[10] M. Kortelainen and J.Suhonen. Microscopic study of muon capture transitions in nuclei involve in double beta decay processes. *Nuclear Physics A*, 2(713):501–521, September 2003. URL http://doi:10.1016/j.nuclphysbps.2005.01.216.

[11] M. Kortelainen and J.Suhonen. Probing double beta decay by nuclear muon capture. *Nuclear Physics B Proceeding Suppl.*, 2(143):551, January 2005. URL http://doi:10.1016/j.nuclphysbps.2005.01.216.

[12] H.Ejiri and M.J.A de Voigt. *Gamma-Ray and Electron Spectroscopy in Nuclear Physics*. Oxford Science Publications, Oxford, NY, 1989.

[13] J.Schweiger et al. Double beta decay to excited states in 76ge within renormalized qrpa. *Journal of Physics G: Nuclear and Particle Physics*, 23(11):1647, November 2012. URL http://doi:10.1088/0954-3899/23/11/012.

[14] H.Ejiri. Isospin core polarization and charge exchanged giant resosnances. *Research Report of Laboratory of Nuclear Science*, 5(1):261–271, 1972.

[15] H.Ejiri. Muon induced reaction for gamma-rays spectroscopy. *Meson*, (39):44–49, 2014.

[16] Hiroyasu Ejiri and I.H.Hashim et. al. Nuclear gamma rays from stopped muon capture reactions for nuclear isotope detection. *Journal of Physical Society Japan*, 82 (044202):1–5, March 2013. URL http://dx.doi.org/10.7566/JPSJ.82.044202.

[17] D.F. Measday. The nuclear physics of muon capture. *Physics Reports*, 354:243–409, December 2001.

[18] K.Ninomiya et. al. Development of elemental analysis by muonic x-ray measurement in j-parc. *Journal of Physics:International Symposium on Advanced Science Research 2009*, 225(012040):1–4, 2010.

[19] G.L. Borchert et. al. High precision spectroscopy of pionic and muonic x-rays to extract an upper limit for the muon-neutrino mass. *Acta Physica Polonica B*, 29: 131–139, 1998.

[20] P.Singer. *Emission of particles following muon capture in intermediate and heavy nuclei*. Haifa, Israel, 1973.

[21] R.Engfer et. al. Charge-distribution parameters, isotope shifts,isomer shifts and magnetic hyperfine constants from muonic atoms. *Atomic Data and Nuclear Data tables*, 14(5):509–597, 1974.

[22] G.R.Lucas and Jr. P. Martin et al. Neutron emission following muon capture in ^{142}ce, ^{140}ce, ^{138}ba and ^{120}sn. *Physical Review C*, 7(4):1678–1686, April 1973.

[23] V.Devanathan. *Observable in nuclear muon capture*. World Scientific, Osaka, Japan, 1989.

[24] F.Myhrer S.I.Ando and K.Kubodera. Capture rate and neutron helicity asymmetry for ordinary muon capture on hydrogen. *Physical Review C*, 63(015203):1–7, December 2000. URL http://doi:10.1103/PhysRevC.63.015203.

[25] P.Vogel. Muonic cascade:general discussion and application to the third row elements. *Physical Review A*, 22(4):1600–1609, October 1980.

[26] Nimai C. Mukhopadhyay. Nuclear muon capture. *Physics Reports*, 30(1):1–144, July 1977.

[27] Glenn F.Knoll. *Radiation detection and measurement*. John Wiley and Sons Inc., Michigan, USA, 2003.

[28] W.R.Leo. *Techniques for nuclear and particle physics experiment*. Springer-verlag Publications, Switzerland, 1994.

[29] H.Ejiri and I.H.Hashim. et. al. Nuclear weak responses by measuring gamma rays from muon capture reactions. Proposal for MLF J-PARC, 2013.

[30] N.Kudomi and T.Shima et al. Preparation of large and thin source films for studying nuclear rare decays. *Nuclear Instruments and Methods in Physics Research A*, 322: 53–56, April 1992.

[31] P. Bossew. A very long-term hpge-background gamma spectrum. *Applied Radiation and Isotopes*, 62:635–644, 2005.

[32] E.Browne and J.K.Tuli. Nuclear data sheets for a=99*. *Nuclear Data Sheets*, 112: 275–446, 2011.

[33] Balraj Singh. Nuclear data sheets update for a=98*. *Nuclear Data Sheets*, 67: 693–807, 1992.

[34] N.Nica. Nuclear data sheets for a=97*. *Nuclear Data Sheets*, 111:525–716, 2010.

[35] D. Abriola and A.A.Sonzogni. Nuclear data sheets for a=96*. *Nuclear Data Sheets*, 109:2501–2655, 2008.

[36] G.Mukherjee S.K. Basu and A.A.Sonzogni. Nuclear data sheets for a=95*. *Nuclear Data Sheets*, 111:2555–2737, October 2010.

[37] Herbert R. Faust. Fragment excitation, kinetic energy distributions and neutron evaporation in nuclear fission calculated from a random excitation model. *International Journal of Modern Physics E*, 13(1):1–6, Oct 2003.

[38] R.Raphael and H.Uberall et al. Neutron emission following muon capture in 16 o. *Physics Review Letters B*, 24(1):15–18, December 1966.

[39] MacDonald and S.N. Kaplan et al. Neutrons from negative muon capture. *Physical Review*, 139(5B):1253–1263, September 1965.

[40] S.Charalambous. Nuclear transmutation by negative stopped muons and the activity induced by the cosmic-ray muons. *Journal of Nuclear Physics A*, 166:145–161, July 1971.

[41] H.J.Evans. Gamma rays following muon capture. *Nuclear Physics A*, (207):379–400, March 1972.

[42] Balraj Singh. Nuclear data sheets for a=100*. *Nuclear Data Sheets*, 109:297–516, 2008.

[43] Hiroyasu Ejiri and Tatsushi Shima. Resonant photo nuclear isotope detection using medium-energy photon beam. *Physical Review Special Topics - Accelerator and Beams*, 15(024701):1–6, Feb 2012. URL http://dx.doi.org/10.1103/PhysRevSTAB.15.024701.